2014

Solid State 1 H Spin - lattice Relaxation and Isolated - Molecule and Cluster Electronic Structure Calculations in Organic Molecular Solids: The Relationship Between Structure and Methyl Group and t - Butyl Group Rotation

Xianlong Wang

Frank B. Mallory

Clelia W. Mallory

Hosanna R. Odhner

Peter A. Beckmann
Bryn Mawr College, pbeckman@brynmawr.edu

Citation

Solid state 1H spin-lattice relaxation and isolated-molecule and cluster electronic structure calculations in organic molecular solids: The relationship between structure and methyl group and t-butyl group rotation. X Wang, F B Mallory, C W Mallory, H R Odhner,* and P A Beckmann 2014 J Chem Phys 140 194304 1-15.

AIP | The Journal of Chemical Physics

Solid state 1H spin-lattice relaxation and isolated-molecule and cluster electronic structure calculations in organic molecular solids: The relationship between structure and methyl group and t-butyl group rotation

Xianlong Wang, Frank B. Mallory, Clelia W. Mallory, Hosanna R. Odhner, and Peter A. Beckmann

Citation: The Journal of Chemical Physics **140**, 194304 (2014); doi: 10.1063/1.4874157
View online: http://dx.doi.org/10.1063/1.4874157
View Table of Contents: http://scitation.aip.org/content/aip/journal/jcp/140/19?ver=pdfcov
Published by the AIP Publishing

Solid state ^{1}H spin-lattice relaxation and isolated-molecule and cluster electronic structure calculations in organic molecular solids: The relationship between structure and methyl group and *t*-butyl group rotation

Xianlong Wang,[1,a)] Frank B. Mallory,[2] Clelia W. Mallory,[2,3] Hosanna R. Odhner,[4,b)] and Peter A. Beckmann[4,a)]

[1]*Key Laboratory for NeuroInformation of Ministry of Education, School of Life Science and Technology, University of Electronic Science and Technology of China, 4 North Jianshe Rd., 2nd Section, Chengdu 610054, China*
[2]*Department of Chemistry, Bryn Mawr College, 101 North Merion Ave., Bryn Mawr, Pennsylvania 19010-2899, USA*
[3]*Department of Chemistry, University of Pennsylvania, Philadelphia, Pennsylvania 19104-6323, USA*
[4]*Department of Physics, Bryn Mawr College, 101 North Merion Ave., Bryn Mawr, Pennsylvania 19010-2899, USA*

(Received 2 February 2014; accepted 18 April 2014; published online 19 May 2014)

We report *ab initio* density functional theory electronic structure calculations of rotational barriers for *t*-butyl groups and their constituent methyl groups both in the isolated molecules and in central molecules in clusters built from the X-ray structure in four *t*-butyl aromatic compounds. The X-ray structures have been reported previously. We also report and interpret the temperature dependence of the solid state ^{1}H nuclear magnetic resonance spin-lattice relaxation rate at 8.50, 22.5, and 53.0 MHz in one of the four compounds. Such experiments for the other three have been reported previously. We compare the computed barriers for methyl group and *t*-butyl group rotation in a central target molecule in the cluster with the activation energies determined from fitting the ^{1}H NMR spin-lattice relaxation data. We formulate a dynamical model for the superposition of *t*-butyl group rotation and the rotation of the *t*-butyl group's constituent methyl groups. The four compounds are 2,7-di-*t*-butylpyrene, 1,4-di-*t*-butylbenzene, 2,6-di-*t*-butylnaphthalene, and 3-*t*-butylchrysene. We comment on the unusual ground state orientation of the *t*-butyl groups in the crystal of the pyrene and we comment on the unusually high rotational barrier of these *t*-butyl groups. © *2014 AIP Publishing LLC*. [http://dx.doi.org/10.1063/1.4874157]

I. INTRODUCTION

Modeling the relationship between structure (molecular and crystal) and internal rotation in molecules and solids provides a better understanding of intramolecular and intermolecular interactions. Bringing together X-ray diffraction,[1] density functional theory *ab initio* electronic structure calculations,[2] and solid state ^{1}H nuclear magnetic resonance (NMR) relaxation,[3] we have previously investigated the relationship between structure (both molecular and crystal) and methyl group rotation in small methyl-substituted planar aromatic organic molecules in the solid state.[4–10] Here we extend these studies to the case of *t*-butyl systems.

In order to calculate barriers for internal rotation in the solid state, clusters of molecules are built from the X-ray structure and ground state cluster energies are computed. A rotor on a central molecule of the cluster is rotated, other nearby atoms are allowed to structurally relax, and the cluster energy is recalculated. In this manner, the energy of a cluster of molecules in the rotational ground state and the energy of the same cluster in a rotational transition state can be calculated. The difference between these two energies is associated with the barrier V for the rotation in question and includes both intramolecular and intermolecular contributions to the barrier. These calculated barriers are then compared with observed solid state ^{1}H NMR activation energies E. The measured E and the calculated V are not the same parameter[11,12] and this comparison requires some discussion.

These studies provide insight into the relationship between the parameters that characterize intramolecular rotation and the parameters that characterize the molecular and crystal structure. They also provide insight into the relative importance of intramolecular bonded interactions, intramolecular electronic (hyperconjugation[13–15]) and steric interactions, and intermolecular interactions that are dominated by van der Waals forces.[16]

Although this is the first report, to our knowledge, of electronic structure calculations for the rotation of a *t*-butyl group *and* its constituent methyl groups, a considerable literature relating solid state ^{1}H spin-lattice relaxation rate experiments and X-ray diffraction exists for these systems. The NMR relaxation experiments involving *t*-butyl group rotation

[a)]Authors to whom correspondence should be addressed. Electronic addresses: WangXianlong@uestc.edu.cn and pbeckman@brynmawr.edu
[b)]Present address: The Vanguard Group Inc., Mailport 8C8, P. O. Box 110, Paoli, Pennsylvania 19482-1110, USA.

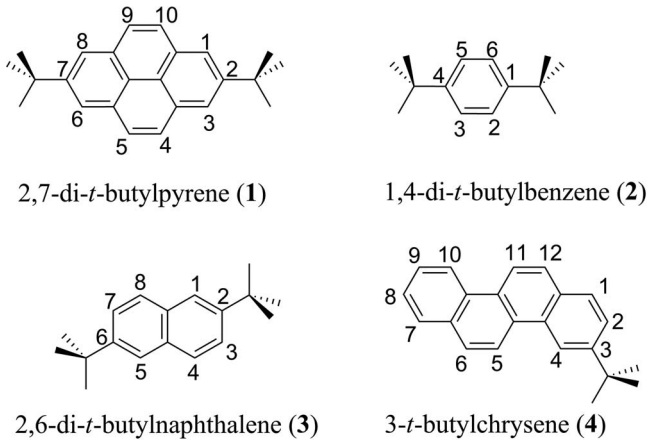

FIG. 1. Schematic pictures of the four compounds investigated in this work. The orientations of the *t*-butyl groups correspond to the calculated ground state structures of the isolated molecules. For **1** and **2**, the *cis* (shown) and *trans* (not shown) conformations differ only slightly in energy. The *t*-butyl groups in the ground state of **1** in the crystal are each rotated approximately 30° from that found in the isolated molecule leaving one methyl group approximately perpendicular to the ring. The *t*-butyl groups in the crystal of **1** are in the *trans* conformation, not the *cis* conformation. The ground state structure of **2** in the crystal is similar to the structure in the isolated molecule in that one methyl group is approximately in the aromatic plane except that the *t*-butyl groups are in the *trans* conformation, not the *cis* conformation as shown here. The ground state structures of **3** and **4** in the crystal are approximately the same as in the isolated molecule. For **1**, **2**, and **3**, the asymmetric unit in the crystal is $Z' = 1/2$. For **4**, $Z' = 1$.

in polycrystalline samples usually show more than one rotor environment (i.e., more than one value of E) as expected[17–26] and usually (but not always[18,22]) the NMR ^{1}H relaxation rate data have a unique interpretation.

The four compounds investigated, shown in Fig. 1, are 2,7-di-*t*-butylpyrene (**1**), 1,4-di-*t*-butylbenzene (**2**), 2,6-di-*t*-butylnaphthalene (**3**), and 3-*t*-butylchrysene (**4**). The rotational dynamics in **1** are probed via solid state ^{1}H NMR spin-lattice relaxation experiments that are reported here. The ^{1}H NMR spin-lattice relaxation experiments have been previously reported for **2**,[24] **3**,[25] and **4**.[23] The crystal structures have been reported elsewhere for all four compounds: **1**,[27] **2**,[28] **3**,[25,29] and **4**.[23]

It is the *inter*molecular interactions that present the computational challenge in this study.[2,30] The state of the art is that electronic structure calculations cannot predict crystal structures very accurately, though matters are improving rapidly.[30,31] We began by building appropriate clusters of 9–14 molecules based on the crystal structure determined by X-ray diffractometry for the ground state structures. (The positions of the H atoms are always calculated since X-ray diffraction does not place H atoms accurately.[32,33]) That is to say, the X-ray experiments provide the initial step in the calculation. We have fixed the positions of the aromatic carbon atoms in all the molecules in a cluster at their X-ray positions. However, we have allowed all the carbon atoms in the *t*-butyl groups and all the hydrogen atoms on all the molecules of the cluster to structurally relax when determining energies in *t*-butyl group and methyl group rotational ground and transition states. We discuss the possible consequences of this simplification.

II. EXPERIMENTAL METHODS

A. Synthesis of 2,7-di-*t*-butylpyrene (1)

A mixture of pyrene (4.0 g, 0.02 mole), anhydrous *t*-butyl alcohol (3.7 g, 0.05 mole), and 60 ml of trifluoroacetic acid was heated at reflux for 15 h. Analysis of the crude reaction mixture by gas chromatography-mass spectrometry (GC-MS) indicated that the majority of the sample was the desired di-*t*-butylpyrene (M^+ 314) with unreacted pyrene (M^+ 202) and a mono-*t*-butylpyrene (M^+ 258) also present. After work up the crude material was recrystallized first from hexanes and then twice from 2:1 benzene-ethanol to give 0.5 g of very small ivory needles with mp 200–202 °C (lit[34] mp 206–208 °C); ^{1}H NMR ($CDCl_3$, 300 MHz) δ 8.18 (s, 4H), 8.02 (s, 4H), 1.55 (s, 18H); GC-MS *m*/*z* 314 (M^+).

B. Electronic structure calculations in the isolated molecules.

The isolated molecular models of 2,7-di-*t*-butylpyrene (**1**), 1,4-di-*t*-butylbenzene (**2**), 2,6-di-*t*-butylnaphthalene (**3**), and 3-*t*-butylchrysense (**4**) were built with the aid of GaussView 3.0 (Gaussian, Inc., Wallingford, CT). All quantum mechanical electronic structure calculations were carried out using the Gaussian09 software package[35] running on a Linux computer cluster. Geometry optimization was performed to obtain the ground state which was used as the starting point for other calculations. Calculations were done at multiple computational levels[2] and the results were consistent across the different levels. Only the results at the B3LYP/6-311+G(*d*,*p*) level are reported here. Potential energy surfaces for the internal rotations (methyl group and *t*-butyl group) were obtained by scanning the relevant internal rotation coordinate while optimizing all other structural parameters. Normal mode analysis at the corresponding computational level was used to confirm the energy minimum and transition points obtained from the scans. Rotational barriers were taken as the difference between the energy of the molecule in the rotational transition state and the energy of the molecule in the rotational ground state.

The internal rotation coordinates for *t*-butyl groups were defined as the dihedral angle formed by three successive bonds: one of the Ct–Cm bonds (where Ct refers to the quaternary C atom in a *t*-butyl group and Cm refers to a constituent methyl group C atom), the *t*-butyl group rotation axis bond, and one of the two aromatic ring C–C bonds flanking the *t*-butyl group rotation axis (see Fig. 1). The choice between the two aromatic ring C–C bonds is arbitrary so long as the aromatic ring remains planar. This is the case for the isolated molecules. In the crystal, however, the aromatic rings are not planar so care must be taken to be consistent when providing dihedral angles in both ground and transition states.

C. Electronic structure calculations in the clusters

We use the cluster approach to partially determine ground state structures and to determine methyl group and *t*-butyl group barriers in the crystalline state. The strengths and weaknesses of the cluster approach and a comparison with the

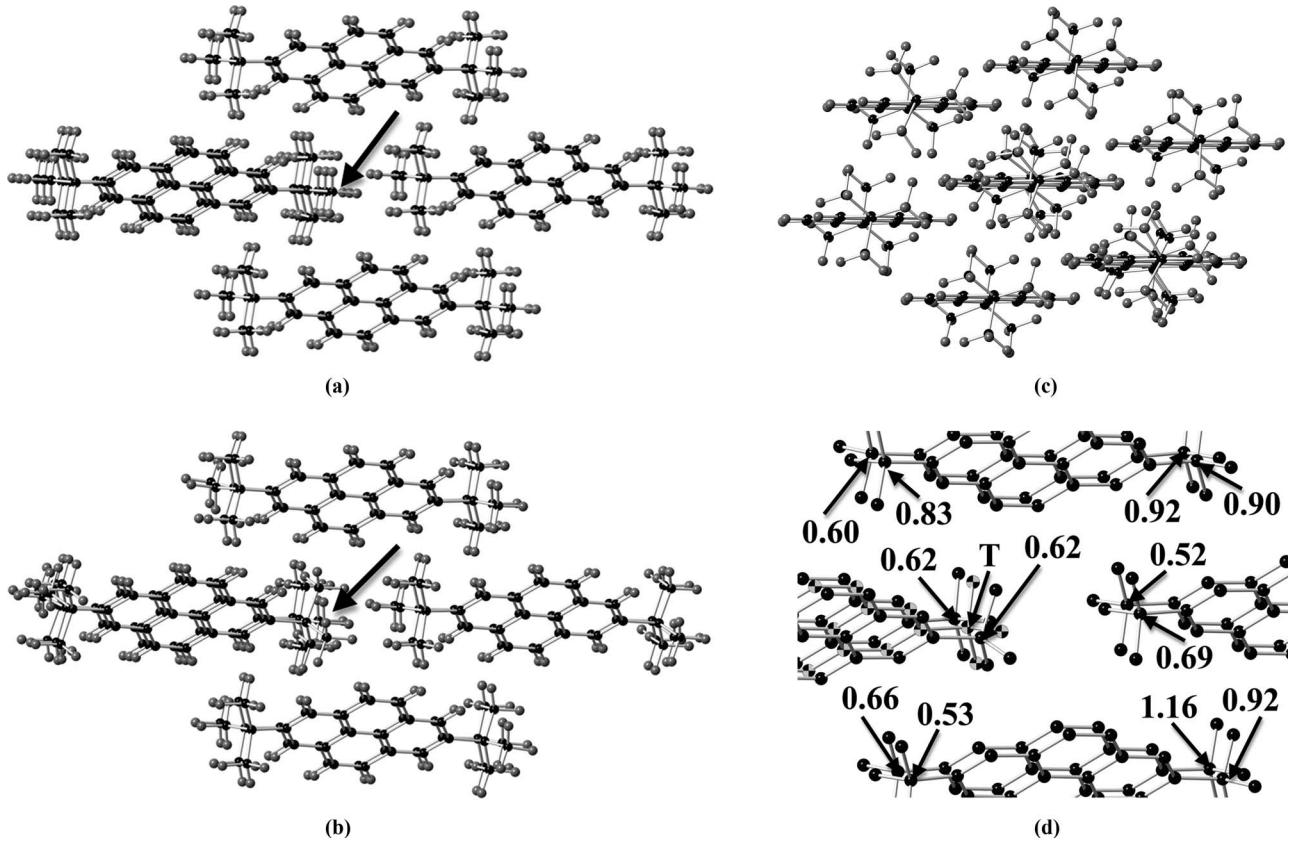

FIG. 2. The 9-molecule cluster of 2,7-di-*t*-butylpyrene (**1**) built from the X-ray structure.[27] C atoms are black and H atoms are grey. (a) Before any calculations are performed. All 9 molecules are visible. The target *t*-butyl group is in the middle of the group of the three indicated by the arrow. (b) The same view as in (a) but after calculations were performed to determine the ground state structure of the cluster. (c) The same cluster as in (b) but rotated by approximately 90° about a vertical axis. (d) A magnification of the central portion of (b) with the H atoms removed for clarity. The target molecule C atoms are indicated as beach balls and the target *t*-butyl group quaternary C atom is indicated by a "T." The distances, in nm, from the target *t*-butyl group quaternary C atom to 12 neighboring *t*-butyl group quaternary C atoms are indicated.

periodic boundary condition (PBC) approach are given in Sec. III. The cluster models of **1**–**4** used to simulate the crystal packing environment of the *t*-butyl groups are indicated in Figs. 2–5. They were constructed from the single-crystal X-ray diffraction data. The reference codes in the Cambridge Crystallographic Structural Database are BUTPYR10 for **1**[27] BUTBNZ for **2**,[28] KOKQUW for polymorph A of **3**,[25,29] and QEFBAE for **4**.[23] The clusters consist of 9–14 molecules and are sufficiently large to include the significant intermolecular interactions between the target *t*-butyl group and the surrounding molecules (as discussed further in Sec. III). Since the two *t*-butyl groups in the crystals of **1**, **2**, and **3** are equivalent (i.e., $Z' = 1/2$), only one cluster model was built for each crystal. There is only one *t*-butyl group in **4** so only one cluster was needed for it as well. Two polymorphs, A and E, of **3** are known[25,29] and only polymorph A is studied in this work.

Because the hydrogen atoms are not accurately positioned in the single-crystal X-ray crystallography experiments,[32,33] a partial structural optimization for all H atoms in each cluster was first performed at the B3LYP/6-31G(*d*) level while freezing all other atoms (which means C atoms in this study). Two computational models, both at the B3LYP/6-31G(*d*) level, called the *rigid rotation model* and the *partial relaxation rotation model*, were used to calculate the barriers for the rotation of the *t*-butyl groups and their constituent methyl groups. The *rigid rotation model* potential energy surface was obtained by single-point calculations while rotating only the specific *t*-butyl group or the specific methyl group in steps of 15° from 0° to 180°. Additional points were calculated around the *rigid rotation model* ground state and transition state for every 2° of rotation. The ground and transition states identified in this manner were subject to the *partial relaxation rotation model* calculation which was carried out in two steps. In the first step, the structural parameters specifying the positions of the H and C atoms in the *t*-butyl group(s) in the home molecule and the positions of all the ring H atoms on the home molecule in the cluster were optimized while the other atoms (the ring C atoms on the home molecule and all atoms in all other molecules) in the cluster were frozen. We called this computational model (which is a subset of the *partial relaxation rotation model*) the *intramolecular relaxation model*. In the second step, the structural parameters specifying the positions of the C and H atoms in all the *t*-butyl groups and the positions of all the H atoms in the clusters were optimized, i.e., only the aromatic ring C atoms on every molecule in the cluster were frozen. We called this computational model the *intermolecular relaxation model*. The basis set superposition error (BSSE)[2,36] was not corrected for in any of these models because of the high computational cost and this is discussed further in Sec. III.

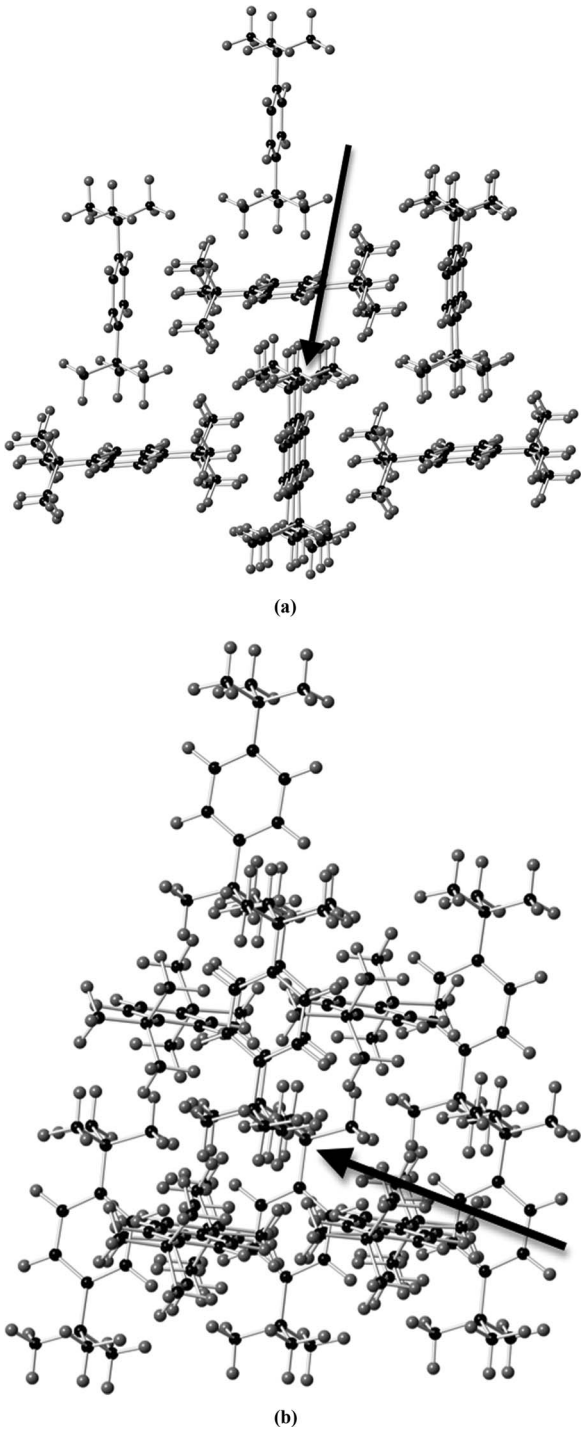

FIG. 3. The 13-molecule cluster of 1,4-di-*t*-butylbenzene (**2**) built from the X-ray structure[28] after calculations were performed to determine the ground state structure. C atoms are black and H atoms are grey. (a) All 13 molecules are visible in this view. The target *t*-butyl group is in the middle of the group of three *t*-butyl groups indicated by the arrow. (b) A view obtained by a rotation of approximately 90° about a vertical axis from the view in (a). The target *t*-butyl group quaternary C atom is indicated by the arrow. One of the target *t*-butyl group's methyl groups is directly above the arrow head.

D. ^{1}H Spin-lattice relaxation

^{1}H spin-lattice relaxation rate R measurements have been reported previously in **2**,[24,26] **3**,[25] and **4**.[23] The rates R were measured in **1** at NMR frequencies of $\omega_N/2\pi = 8.50$, 22.5, and 53.0 MHz between 100 and 360 K and are presented in Fig. 6. *Low* NMR frequencies are needed to bring the various rotations into resonance with the NMR frequency in reasonable temperature ranges. The rates were measured with an inversion-recovery pulse sequence and the decay of the magnetization $M(t)$ for time t between the perturbation and measurement pulses was found to be exponential over the entire temperature range at all three NMR frequencies. At 53.0 and 22.5 MHz, the S/N was large and the exponentiality of the decay was checked very carefully by observing $M(t) - M(\infty)$ over three orders of magnitude and fitting the decay to both a single exponential and a stretched exponential as discussed extensively in Ref. 6. The variable-temperature system, temperature control, temperature measurement, and temperature reproducibility are discussed in Ref. 6. Although the free induction decay in these kinds of solids is not strictly exponential,[37] here it was approximately so, with the

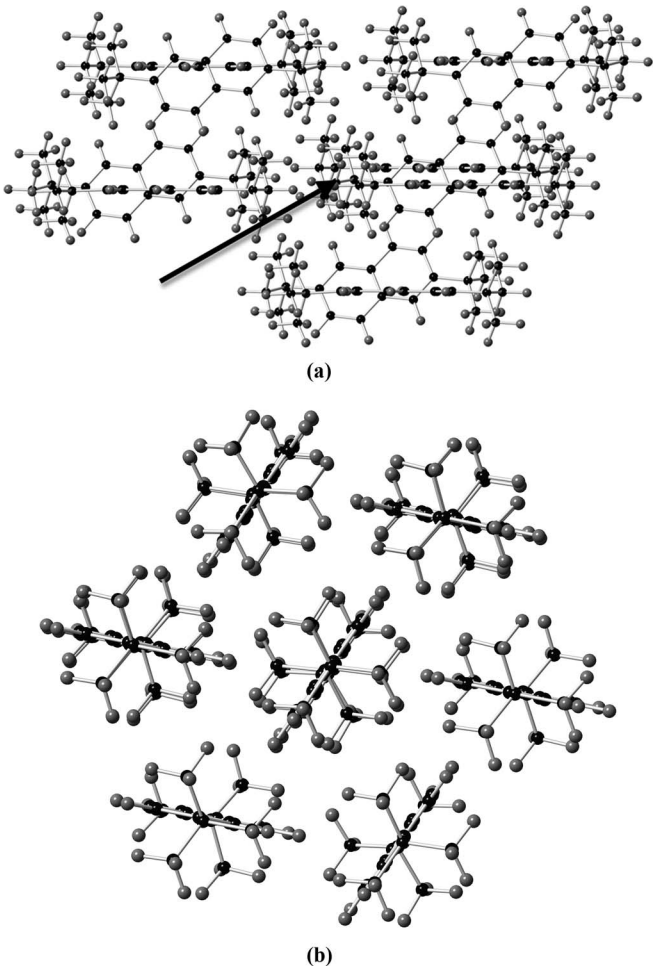

FIG. 4. The 11-molecule cluster of polymorph A of 2,6-di-*t*-butylnaphthalene (**3**) built from the X-ray structure[25,29] after calculations were performed to determine the ground state structure. C atoms are black and H atoms are grey. (a) All molecules are visible; four in the top row, five in the middle row (two to the left and three to the right), and two in the bottom row. The target molecule is in the center (into the page) of the three molecules to the right in the center row. The target *t*-butyl group is indicated by the arrow. (b) A view obtained by a rotation of approximately 90° about a vertical axis from the view in (a). This view shows that the aromatic rings are oriented in one or the other of two orientations. Only the "front" seven molecules of the 11-molecule cluster are visible and the target *t*-butyl group is hidden into the page behind the central molecule shown.

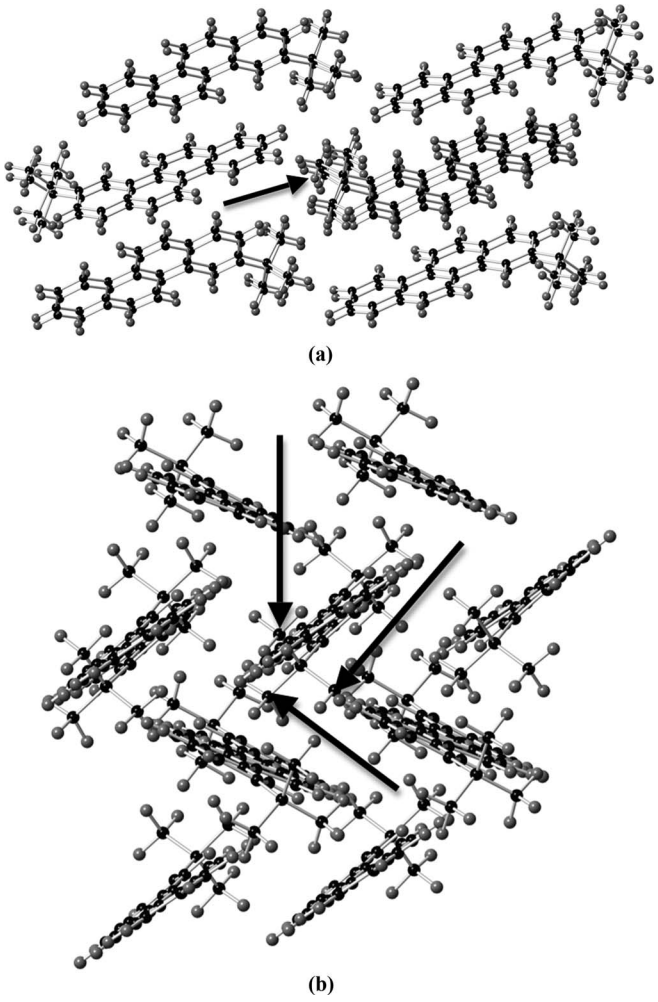

FIG. 5. The 13-molecule cluster of 3-*t*-butylchrysene (**4**) built from the X-ray structure[23] after calculations were performed to determine the ground state structure. C atoms are black and H atoms are grey. (a) A view with all molecules visible and where the target *t*-butyl group is indicated by the arrow. (b) A view where the chrysene backbone (which is not planar) is seen end on. The three methyl group C atoms on the target *t*-butyl group are visible and are indicated by the three arrows.

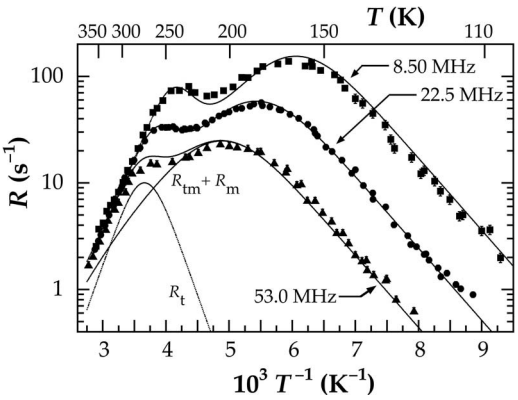

FIG. 6. The ^{1}H spin-lattice relaxation rate R in polycrystalline 2,7-di-*t*-butylpyrene (**1**) as a function of temperature T at three NMR frequencies as shown. The single fit to all three frequencies is discussed in Secs. IV and V D. $R = R_t + R_m + R_{tm}$ (Eq. (3)) and the contribution of the first term and sum of the contributions of the latter two terms are shown for 53.0 MHz.

spin-spin relaxation time $T_2 \approx 7\ \mu$s, making measurements at 8.50 MHz difficult since the amplifier recovery time is quite long at this low NMR frequency. The uncertainties on the 22.5 and 53.0 MHz R values, and on the 8.50 MHz R values above 140 K are taken as $\pm 6\%$, much larger than the uncertainties returned by least squares fitting routines. The uncertainties on the 8.50 MHz values below 140 K (where T_2 becomes even smaller as the line broadens further) are taken as $\pm 10\%$. These uncertainties are realistic and meaningful and are arrived at by analyzing contrived data with various amounts of random noise.[38] A few error flags can be seen outside the sizes of the symbols (at 8.50 MHz at low temperature) used in Fig. 6.

III. CHOICE OF COMPUTATIONAL MODELS

There are two possible approaches that can be used to study methyl group and/or *t*-butyl group rotation in crystalline solids: the cluster approach and the periodic boundary conditions (PBC) approach. In the cluster approach used in this study, a cluster consisting of several neighboring molecules in the vicinity of a home molecule is considered in order to represent the local environment for the home molecule in the crystal. The geometry of the cluster model can be obtained either from the X-ray diffraction structure as done in this study or it can be built using quantum chemical calculations. The main advantage of the cluster approach is that the recently developed accurate and advanced quantum chemical methods, such as RI-MP2,[39] can be applied to the system. The cluster approach has been successfully used by us[4,5,7–9] and others[39] to study the rotation of methyl groups in crystals, the vibration modes of methyl groups on surfaces,[40] and hydrogen-bonded ammonia clusters.[41] In addition, the analytical second derivative of the potential energy surface is available for a normal mode analysis.

There are two potential limitations to the cluster approach. The first is that only the microenvironment experienced by the target rotor on the home molecule accurately reflects the crystalline environment. Other rotors would experience an artificial environment in that they may be too close to the edge of the cluster (Figs. 2–5). This potential limitation is not a problem so long as the cluster size is large enough to include all the close neighbors which have a significant impact on the rotation of the target rotor. That is, if the cluster is not large enough, there may be edge effects on the target rotor as a result of the exclusion of very long range interactions. However, when we systematically build larger and larger clusters and calculate the rotational barrier for the target rotor, we find that the barrier converges when the cluster size reaches approximately 9–13 molecules, depending on the shape and size of the molecules in question. This usually includes all the molecules with a shortest distance from their center of mass to the target rotor of approximately 0.7–0.8 nm.[42] From a different perspective, this potential limitation actually presents two advantages. As shown by scanning electron microscopy (SEM),[5] some polycrystalline solids studied using NMR relaxation methods have either a significant surface area or crystal defects or both, which means that some rotors would have a different environment from the ideal crystal environment.

These can be simulated in the cluster model and we are proceeding with such studies. A detailed analysis needed to determine which interactions contribute to the rotational barrier of the target molecule is also conveniently performed by the selective inclusion of neighboring molecules in the cluster.[42]

The second potential limitation of the cluster model in the crystals we study is that the dominant contribution to the intermolecular interactions is weak van der Waals interactions[16] and the clusters might fall apart in a full geometry optimization if there were no constraints. We have solved this problem in most cases by fixing the aromatic backbone atoms at their X-ray measured equilibrium positions and we have allowed only other atoms to relax. However, some aromatic C atoms can be allowed to relax in special cases, as in the example of benzene ring rotation presented in Sec. V C 4. Indeed, the cluster method is very versatile in this respect. Another potential limitation which might be encountered in studying covalent bonded solids is the appearance of dangling bonds due to cluster truncation. This is not a problem in the way we use the cluster method since we always include whole molecules in the clusters.

In the periodic boundary condition (PBC) approach, a unit cell is repeated in the three dimensional space with full periodicity and density functional methods are usually used to perform the calculations. This model allows all the rotors to experience the effects of the intermolecular interactions in an ideal crystal. Plane wave basis sets are popular in the PBC approach, yet for the molecular crystals, the localized Gaussian-type functions are more appropriate.[43] However, the Gaussian basis sets used in molecular studies cannot be directly applied in the PBC calculations. Diffuse functions are often necessary in order to describe the long range decay of the wave function for the isolated molecules.[44] Yet, for the PBC calculations, the inclusion of diffuse functions in the Gaussian basis sets causes a serious linear dependence problem in that some of the resulting basis functions are inappropriately dependent on one another. The inclusion of diffuse basis functions in the Gaussian basis sets also results in a large BSSE. Therefore, the molecular Gaussian basis sets need to be re-optimized for the PBC calculations.[45,46] Although the PBC approach seems more natural to simulate the extended crystal systems, the computational cost is prohibitive because the primitive unit cell would be very large for the crystals studied here. A super cell consisting of two or more neighboring unit cells is often needed in the PBC calculations in order to avoid the spurious rotational coupling between the neighboring cells. DFT methods that include exact exchange (Hartree-Fock), e.g., B3LYP, and other post-HF methods that can be applied in the cluster approach, are often not feasible in the PBC approach. Another major limitation to the PBC calculations is that the analytical second derivative technique is often not available and a normal node analysis is expensive. The frequency calculation is often carried out numerically at the Γ point only, instead of sampling the first Brillouin zone extensively. This assumes that the displacements of all the atoms in the unit cell are the same. Therefore, for the purpose of studying the dynamics of *t*-butyl group and/or methyl group rotation, the cluster model is a more reasonable choice in practice.

It is important to include London dispersion forces in modeling molecular crystals when the intermolecular interactions are dominated by van der Waals forces. (The London dispersion forces are one of several forces that come under the umbrella of van der Waals forces.[16]) The calculation of London dispersion interactions is a very difficult task and most DFT methods, including B3LYP (which we use in this study), do not treat the long-range London dispersion forces correctly.[47,48] Understanding the consequences of this is an active area of research. Correction methods for the calculation of London dispersion forces, such as the DFT-Dx (x = 1, 2, and 3) method and the exchange-hole dipole moment (XDM) model have been developed.[47,49] These corrections have been shown to be important in order to improve the calculation of crystal geometries and sublimation enthalpies. Whether the correction for the inclusion of London dispersion forces affects the rotational barrier calculation has not yet been determined and this will be included in our future studies. Our choice of the B3LYP/6-31G(*d*) theory model used in the cluster calculations has produced reliable methyl group rotational barriers that are in reasonable agreement with solid state NMR relaxation experiments.[4,5,7–9] The success of our method in calculating barrier heights is presumably due to the cancellation of the systematic error resulting from neglecting the long-range London dispersion interaction. The rotation of the target methyl or *t*-butyl group in the cluster disturbs the whole cluster geometry only slightly and the possible systematic error on the total energy would be largely canceled out when calculating a barrier: that is, when calculating the difference between the ground state and the transition state energies.

Another potential concern of the cluster model is the BSSE,[2] which may be responsible for unreliable results, particularly in studying van der Waals systems and hydrogen-bonded complexes.[41] The counterpoise method is often used to correct this error in small-to-medium size systems. A detailed analysis on a dimer of 3-(trifluoromethyl)phenanthrene shows that the BSSE contributes about only 10% to the barrier height of the rotation of the trifluoromethyl group, thanks, again, to a systematic error cancellation.[9] The uncertainties resulting from the BSSE are about the same scale as the uncertainty of our computational results and therefore the BSSE is not corrected due to the significant additional computational cost of the counterpoise method when applied to our systems. Recently, an empirical geometrical counterpoise ("gCP") correction method for large systems has been reported.[50] We applied the gCP method in a cluster and found the effect of the BSSE correction to be approximately 0.5 kJ mol^{-1} to the methyl group rotational barrier, though the overall correction was more than 1.8 MJ mol^{-1} for an entire cluster. The final correction to the barrier has gone beyond the accuracy of the gCP method itself and as such we do not use it in this study.

IV. NMR ^{1}H SPIN-LATTICE RELAXATION REVIEW AND THE RELAXATION RATE PARAMETERS FOR 2,7-DI-*t*-BUTYLPYRENE

The basic model for ^{1}H spin-lattice relaxation resulting from the modulation of the spin-spin (dipolar) interaction

(for spin 1/2 particles) was developed[37,51–58] and then extended[59–62] to the three spins in a methyl group with the motion being methyl group rotation. Hilt and Hubbard,[63] and Runnells[64] showed that the ^{1}H spin-lattice relaxation for a methyl group was inherently nonexponential and nonexponential relaxation has been observed.[6,65–69] The presence of either ^{1}H spin-spin interactions between methyl group ^{1}H spins and other ^{1}H spins or between ^{1}H spins on different methyl groups (in a *t*-butyl group, for example) makes the relaxation more exponential by reducing the effect of the correlations that are responsible for the nonexponential relaxation.[66,69] This has been born out in experiments with solids comprised of larger organic molecules with several or many static (on the NMR time scale) H atoms. If methyl group rotation is superimposed on other motions that are also on the NMR time scale, then again the relaxation becomes more exponential.[70] This is the case for methyl group rotation superimposed on *t*-butyl group rotation. For *t*-butyl group systems, the departure from exponential relaxation is very slight or not observed at all to within experimental uncertainty.[18–23,25,26] A calculation of the relaxation rate resulting from methyl group rotation superimposed on several additional rotations has been presented.[71–74] The most general expression for the particular case of a single *t*-butyl group, employing a very helpful and simplifying assumption to deal with intra-*t*-butyl, intermethyl ^{1}H spin–^{1}H spin interactions, was developed by Albert *et al.*[75] The most convenient expression for the ^{1}H spin-lattice relaxation rate for our purposes is[23,26]

$$R = \frac{9}{M} R^{\text{inter}} + \sum_{j=1}^{3} \frac{3}{M} R_j^{\text{intra}}. \tag{1}$$

Equation (1) refers to a single *t*-butyl group in a bath of its own 9 H atoms and $M - 9$ other H atoms. If the asymmetric unit is half a molecule as in **1**, then M is half the number of H atoms in a molecule. R_j^{intra} ($j = 1, 2, 3$ for the three methyl groups in a *t*-butyl group) accounts for the three dipolar interactions among the three ^{1}H spins in the jth methyl group and R^{inter} accounts for the 27 dipolar interactions among the nine ^{1}H spins on different methyl groups in a *t*-butyl group employing the very reasonable simplifying assumption of Albert *et al.*[75] Interactions between *t*-butyl group ^{1}H spins and non-*t*-butyl group ^{1}H spins are not accounted for in Eq. (1) (nor need they be for **1** as discussed in Sec. V D).

To a very good approximation, the mean hopping frequency of a methyl group or a *t*-butyl group is,[76]

$$\tau_i^{-1} = \nu_{i,\infty} e^{-E_i/kT}, \tag{2}$$

for $i =$ t for a *t*-butyl group or $i =$ mj ($j = 1, 2, 3$) for the three methyl groups. T is the absolute temperature and k is Boltzmann's constant. The mean time between hops τ_{t} for a *t*-butyl group is characterized by the NMR activation energy E_{t} and by a preexponential factor $\nu_{\text{t},\infty}$. The mean times between hops for the three methyl groups $\tau_{\text{m}j}$ are characterized by $E_{\text{m}j}$ and $\nu_{\text{m}j,\infty}$, $j = 1, 2, 3$. The ∞ subscript refers to the fact that $\tau_i^{-1} \rightarrow \nu_{i,\infty}$ at $T \rightarrow \infty$. The observation of linear ln$R$ versus T^{-1} at low and high temperatures (as observed here for **1** and elsewhere for **2**,[24] **3**,[25] and **4**[23]) lends further support to the simplifying assumptions leading to Eq. (2).

Above approximately 80 K in most solids, modeling methyl group rotation as a random hopping of the triangle of H atoms using Eq. (2) for the mean hopping rate is an excellent model for the interpretation of ^{1}H NMR spin-lattice relaxation rate data.[4,6,10,17–20,22,23,25,26,77–82] Below approximately 80 K (and certainly by 40 K) methyl group rotation is better described by quantum mechanical tunneling.[83,84] For completeness, we note that the transition from the low-temperature quantum mechanical tunneling regime to the high-temperature semiclassical hopping regime (used here) is well understood.[76–78,80,82,85]

In developing models for relating *t*-butyl group rotation and methyl group rotation to the observed relaxation rates in **1**, we are guided by the simplest possible reasonable model that fits the data; namely, that which has the least number of adjustable parameters (and still makes sense). With this *modus operandi*, we note that all three methyl groups in **1** are "well away" from the plane of the adjacent ring and, to within the precision determined by fitting the NMR relaxation rate data, can be characterized by the same mean time between hops. For **1**, Eq. (1) is written[86]

$$\begin{aligned} R &= R_{\text{t}} + R_{\text{m}} + R_{\text{tm}} \\ &= \frac{1}{M} \left\{ C_{\text{t}} h\left(\omega_{\text{N}}, \tau_{\text{t}}\right) + 3C_{\text{m}} h\left(\omega_{\text{N}}, \tau_{\text{m}}\right) + 3C_{\text{tm}} h\left(\omega_{\text{N}}, \tau_{\text{tm}}\right) \right\}, \end{aligned} \tag{3}$$

where τ_{m} characterizes the hopping of all three methyl groups, τ_{t} characterizes the hopping of the *t*-butyl group, $\omega_{\text{N}}/2\pi$ is the NMR frequency, $M = 13$ (H atoms in half a molecule), and where the C-constants can be expressed in closed form.[23] For **1**, this gives $C_{\text{t}} = 1.58 \times 10^{10}$ s^{-2}, $C_{\text{m}} = 3.92 \times 10^9$ s^{-2}, and $C_{\text{tm}} = 9.31 \times 10^9$ s^{-2}. We note that these C constants use a more accurate value for the H–H distance in a methyl group[20] (determined by the electronic structure calculations in the clusters) than do older publications. In Eq. (3),

$$h\left(\omega, \tau\right) = \frac{2\tau}{1 + \omega^2\tau^2} + \frac{8\tau}{1 + 4\omega^2\tau^2}, \tag{4}$$

and the superposition frequency τ_{tm}^{-1} is[61,62,71–75]

$$\tau_{\text{tm}}^{-1} = \tau_{\text{t}}^{-1} + \tau_{\text{m}}^{-1}. \tag{5}$$

The factors of 3 in Eq. (3) result from the fact that the three methyl groups are taken to be dynamically equivalent. The more general expression has seven terms; one for the *t*-butyl group, three for the three methyl groups, and three involving the superposition of the methyl group and *t*-butyl group mean hopping frequencies. For **1**, the seven terms reduce to the three terms in Eq. (3).

The above analysis means that in **1** there is one activation energy E_{t} for the *t*-butyl group and another $E_1 = E_2 = E_3$ for the methyl groups. An analysis for **2**,[24] **3**,[25] and **4**[23] can be performed in a similar manner. Unlike **1** where all three methyl groups are "well away" from the ring, **2**, **3**, and **4** all have one methyl group in the plane of the ring (or very close to it). This means that the *t*-butyl group and one methyl group

are associated with the same activation energy $E_t = E_1$ that, in a classical description, characterize a geared motion. The other two methyl groups are characterized by another activation energy $E_2 = E_3$. Compound **3** is unusual in that these two activation energies are the same; that is $E_t = E_1 = E_2 = E_3$.

V. EXPERIMENTAL RESULTS

A. Ground state *t*-butyl group orientations derived from the X-ray diffraction experiments

The reference codes in the Cambridge Structural Database are BUTPYR10 for **1**,[27] BUTBNZ for **2**,[28] KOKQUW for polymorph A of **3**,[25,29] and QEFBAE for **4**.[23] In this paper, the following dihedral angles are used to specify the orientational positions of the three methyl groups on the *t*-butyl groups. Ct refers to *t*-butyl group quaternary C atom and Cm refers to a methyl group C atom (see Fig. 1). In **1**, θ (Cm-Ct-C2-C1) and θ (Cm-Ct-C7-C6) are used for the *t*-butyl groups at the 2 and 7 positions. In **2**, θ (Cm-Ct-C1-C2) and θ (Cm-Ct-C4-C5) are used for the *t*-butyl groups at the 1 and 4 positions. In **3**, θ (Cm-Ct-C2-C1) and θ (Cm-Ct-C6-C5) are used for the *t*-butyl groups at the 2 and 6 positions. In **4**, θ (Cm-Ct-C3-C4) is used for the single *t*-butyl group in the 3 position.

Since $Z' = 1/2$ for **1**, **2**, and **3**, it is only necessary to specify the orientation of one *t*-butyl group in characterizing the ground state structure in the solid. In all three cases, the *t*-butyl groups are in the *trans* conformation which, indeed, is implied by $Z' = 1/2$. (Note that the *cis* conformation is shown in Fig. 1 for **1** and **2** because this corresponds to the ground state in the isolated molecules.) In **1**, both *t*-butyl groups in the crystal form a nearly perpendicular conformation. The dihedral angles θ (Cm-Ct-C2-C1) specifying the rotational positions of the three methyl groups in one of the *t*-butyl groups are 96°, −24°, and −145°. This means that one methyl group is approximately 84° from the aromatic plane on one side of that plane and that the other two methyl groups are approximately 24° and 35° from the aromatic plane on the other side of that plane. Thus all three methyl groups are "well away from" the aromatic plane. We refer to this unusual orientation as the "perpendicular" geometry, since one methyl group is essentially perpendicular to the plane of the aromatic ring. Even though the ring is not planar (thus a liberal use of the word "approximately" in specifying some of the angles above), the inversion center is preserved ($Z' = 1/2$). The departure from planarity of the pyrene ring is only a few degrees. The orientation of one of the *t*-butyl groups in the crystal structure of **2** is such that the three methyl groups have dihedral angles of 8°, 128°, and −112°. Thus there is one methyl group in the plane of the aromatic ring (or nearly so) and two methyl groups well out of the plane. The dihedral angles of the three methyl groups in **3** are 0°, 121°, and −119°, and in **4** ($Z' = 1$) they are 2°, 122°, and −119°. The ring system in **4** (the longest among all four aromatic rings and therefore more flexible than the others) becomes slightly twisted in the crystal. For example, the angle C2-C3-C8-C9 is 7.3°. Presumably this twist results from the intermolecular interactions in the crystal.

B. Electronic structure calculations in the isolated molecules

1. Ground state structures

The ground-state molecular structures of the isolated molecules of the four compounds calculated at the B3LYP/6-311++G(*d*,*p*) level are shown in Fig. 1. In each case, a normal-mode analysis was carried out at the same computational level to confirm that the calculated geometry corresponds to a minimum energy conformation. Based on the structural characteristics, the four compounds can be divided into two categories. In **1** and **2**, the aromatic rings are symmetric with respect to the perpendicular plane that goes through the two *t*-butyl group rotational axes and the two aromatic C–C bonds adjacent to the *t*-butyl groups would have equal π bond order if the *t*-butyl groups were absent. In **3** and **4**, this symmetry is not present. In **3**, C1-C2 (and C6-C5) has a higher π bond order than C2-C3 (and C6-C7), and in **4**, C3-C4 has a higher π bond order than C2-C3. For **1**, the *cis* conformation shown in Fig. 1, is 0.4 kJ mol^{-1} lower in energy than the *trans* conformation. For **2**, the *cis* conformation shown in Fig. 1 is 0.5 kJ mol^{-1} lower in energy than the *trans* conformation. In all cases one of three Ct–Cm bonds is coplanar with the corresponding aromatic ring. That is, the three dihedral angles for the three methyl groups in all the *t*-butyl groups in all four molecules can be taken as 0°, 120°, and −120°. These angles can be compared with those found in the X-ray structure presented in Sec. V A.

2. Rotational barriers of t-butyl groups in the isolated molecules

The rotational potential energy surfaces of the *t*-butyl groups computed at the B3LYP/6-311++G(*d*,*p*) level in the isolated molecules of **1**–**4** are plotted in Fig. 7. In Fig. 8, we show the relationship between the angles specifying the *t*-butyl group and the in-plane methyl group. By the time the *t*-butyl group has rotated by 60° (Fig. 8), the in-plane methyl group has become an out-of-plane methyl group (and another out-of-plane methyl group has become the in-plane methyl group on the other side of the ring). Because the barrier for rotation of the in-plane methyl group (presented in

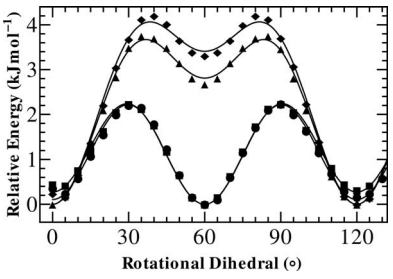

FIG. 7. Fully relaxed potential energy surfaces for the rotation of the *t*-butyl groups calculated at the B3LYP/6-311++G(*d*,*p*) level for isolated molecules of (**1**) 2,7-di-*t*-butylpyrene (●), (**2**) 1,4-di-*t*-butylbenzene (■), (**3**) 2,6-di-*t*-butylnaphthalene (♦), and (**4**) 3-*t*-butylchrysene (▲). At the resolution shown, the curves for **1** and **2** are barely distinguishable. The solid curves are the best-fit of each data set to a two-cosine potential (see Eq. (6)) and the fitting coefficients are given in Table II.

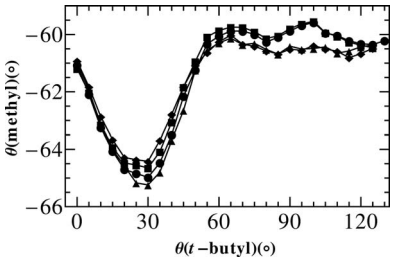

FIG. 8. The in-plane methyl group dihedral angle θ (methyl) versus the *t*-butyl group dihedral angle θ (*t*-butyl) for isolated molecules of (**1**) 2,7-di-*t*-butylpyrene (●), (**2**) 1,4-di-*t*-butylbenzene (■), (**3**) 2,6-di-*t*-butylnaphthalene (♦), and (**4**) 3-*t*-butylchrysene (▲). When θ (*t*-butyl) has reached 60°, the methyl group has become an out-of-plane methyl group. Note that the θ (methyl) range is only approximately 5°.

Sec. V B 3) is significantly greater than the barrier for rotation of the *t*-butyl group (presented in the next paragraph) in the isolated molecule, the in-plane methyl group rotates very little (presumably "gearing" around a ring H atom) as the *t*-butyl group rotates. Note that the range of methyl group angles in Fig. 8 only covers approximately 5°. Indeed, in all four molecules, this methyl group rotates only approximately 5° (and then back again) as the *t*-butyl group rotates to or near its transition state. The potential energy surfaces of **1** and **2** (Fig. 7) have approximately 6-fold symmetry and the perpendicular conformations (corresponding to a rotation of approximately 30° from the ground state) are the transition states. More precisely, in the isolated molecules, the transition states correspond to a rotation of 28.6° in **1** and 29.0° in **2**. At the resolution shown in Fig. 7, the curves for **1** and **2** are barely distinguishable. The potential energy surfaces of **3** and **4** have both 3-fold and 6-fold components so a rotation of approximately 60° from the ground state is not the transition state but an intermediate state (i.e., a local energy minimum) (Fig. 7). The transition state in **3** corresponds to a *t*-butyl group rotation of 39.5° and the transition state in **4** corresponds to a *t*-butyl group rotation of 36.7°.

The barriers to the rotation of the *t*-butyl groups can be divided into two categories as well. **1** and **2** have the smaller barriers, $V_{\text{t, iso}} = 2.2$ kJ mol^{-1}, whereas the barriers in **3** and **4**, $V_{\text{t, iso}} = 4.0$ kJ mol^{-1} and $V_{\text{t, iso}} = 3.8$ kJ mol^{-1}, respectively, are larger. The subscript "t" refers to "*t*-butyl group" and the subscript "iso" refers to "isolated molecule." These values of $V_{\text{t, iso}}$ are indicated in Table I. The four potential energy surfaces in Fig. 7 are well fitted by a sum of two cosine

TABLE II. Barrier amplitudes (in Eq. (6)) for the isolated molecules.[a]

#	Compound	V_3	V_6
	t-butylbenzene	...	2.14(3)
1	2,7-di-*t*-butylpyrene	0.11(3)	2.16(4)
2	1,4-di-*t*-butylbenzene	0.27(3)	2.10(3)
3	2,6-di-*t*-butylnaphthalene	3.41(5)	2.00(5)
4	3-*t*-butylchrysene	2.81(4)	2.02(4)

[a]Energies are in kJ mol^{-1}.

potentials:

$$E = \frac{V_3}{2}(1 - \cos 3\theta) + \frac{V_6}{2}(1 - \cos 6\theta), \qquad (6)$$

where θ is the dihedral angle the in-plane methyl group makes with the plane. The fitting coefficients, V_3 and V_6, are tabulated in Table II. For comparison, the potential energy surface of *t*-butylbenzene was also calculated and the fitting coefficients are also included in Table II. The six-fold terms, V_6, are approximately the same (~2 kJ mol^{-1}) among the five compounds, but the three-fold terms, V_3, vary significantly. The potential energy surface of *t*-butylbenzene has perfect six-fold symmetry. **1** and **2** have a small three-fold component but in **3** and **4**, the V_3 terms are larger than the V_6 terms. The origin of V_3 can be ascribed to the electronic hyperconjugation effect[13–15] whereas the origin of V_6 can be ascribed to steric hindrance.[7] The hyperconjugation effect refers to the "electron redistribution effect" between the *t*-butyl group and the aromatic ring.[13–15] In previous publications, we have referred to this as the "electronic" component of the barrier.[7] Such an effect plays a significant role in the case of methyl rotors.[7] The magnitude of the contribution of the hyperconjugation effect to the rotational barrier is dependent on the π electron density difference between the two aromatic ring C–C bonds connected to the rotational axis. In *t*-butylbenzene, the benzene ring has an equal π electron distribution among the six aromatic C–C bonds. Therefore, the hyperconjugation effect plays no role, and the resultant potential energy surface has perfect six-fold symmetry. The π bond symmetry in **1** and **2** is slightly perturbed due to the presence of the other *t*-butyl group, which reflects the long range effect induced by the hyperconjugation between the aromatic ring and the *t*-butyl group at the *para* position. For example, C1-C2 is shorter than C2-C3 by 0.004 Å in **1** and C1-C6 is shorter than C1-C2 by only 0.0004 Å in **2**. As such, the V_3 term is

TABLE I. Calculated barriers *V* for *t*-butyl and constituent methyl groups in both the isolated molecule and in the solid state.[a]

#	Compound	$V_{\text{t,iso}}$[b]	$V_{\text{t,clust}}$[b,c]	$V_{\text{in,iso}}$[b]	$V_{\text{out,iso}}$[b]	$V_{1,\text{clust}}$[c]	$V_{2,\text{clust}}$[c]	$V_{3,\text{clust}}$[c]	X-ray Refs.
1	2,7-di-*t*-butylpyrene	2.2	33.9	14.6	14.8	19.6	16.6	16.4	27
2	1,4-di-*t*-butylbenzene	2.2	15.5	14.5	14.9	25.5	18.4	17.7	28
3	2,6-di-*t*-butylnaphthalene[d]	4.0	16.3	18.4	14.5	25.1	18.4	16.4	25 and 29
4	3-*t*-butylchrysene	3.8	19.5	17.6	14.7	26.0	18.4	17.7	23

[a]All energies are in kJ mol^{-1}.
[b]"iso" means isolated molecule. "In" means in-plane and "out" means out-of plane methyl. "t" means *t*-butyl.
[c]"clust" means in the cluster. Number subscripts order the methyl group barriers from largest to smallest. These values are compared with the NMR activation energies in Table III.
[d]Only polymorph A is considered for the cluster calculations.

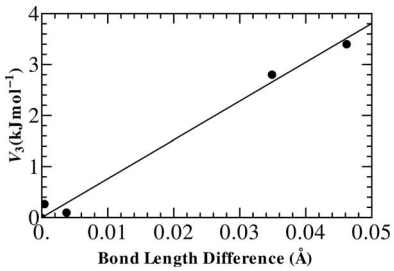

FIG. 9. The 3-fold cosine term fitting coefficient V_3 (indicated in Table II) of the *t*-butyl group rotational potential energy curves (Fig. 7) versus the length difference between the two aromatic C–C bonds adjacent to the *t*-butyl groups. The straight line is the linear best-fit with a slope of 76 ± 3 kJ mol^{-1} Å^{-1}.

very small. However, in **3** and **4**, the naphthalene and chrysene rings do not have equal π electron distribution even in the absence of a *t*-butyl group. The two aromatic C–C bonds adjacent to a *t*-butyl group have significantly different bond lengths as a result. The preferred *t*-butyl group orientation is the one where the Cm–Ct bond is coplanar with the ring on the side with larger π bond order (i.e., shorter bond length) for which the stabilization effect due to the hyperconjugation is stronger. The dependence of the fitting coefficients of the 3-fold term on the bond length difference between the two adjacent aromatic C–C bonds is reasonably well fitted with a straight line as seen in Fig. 9. This bond length difference is a measure of the difference of the π bond order. The steric hindrance is due to the repulsion between the *t*-butyl group H atoms and the two H atoms on the aromatic rings adjacent to the *t*-butyl groups. This leads to the six-fold symmetry. The closest methyl group H–ring H distance is reached at θ (*t*-butyl) = 30°. This shortest distance is approximately 2.09 Å among all the molecules; therefore the V_6 terms are nearly identical.

3. Rotational barriers of the constituent methyl groups in the isolated molecules

For the constituent methyl groups of all the *t*-butyl groups in the isolated molecules of **1**–**4**, the staggered conformation is the ground state and the eclipsed conformation (a rotation of 60°) is the rotational transition state. Because one Cm–Ct bond is coplanar with the aromatic ring in the ground state, the three constituent methyl groups can be divided into one "in-plane" methyl group and two "out-of-plane" methyl groups. The in-plane methyl group has a barrier $V_{\text{in, iso}}$ where the subscript "in" refers to "in the plane" of the aromatic ring and the subscript "iso" refers to the isolated molecule. The other two methyl groups, which are symmetric with respect to the ring (60° above and below), are the out-of-plane methyl groups and they have a barrier $V_{\text{out, iso}}$. The barriers to the rotation of the out-of-plane methyl groups are approximately the same ($\sim$15 kJ mol^{-1}) in the four compounds. The more precise values are indicated in Table I. In **1** and **2**, the barriers to the rotation of the in-plane methyl groups are approximately the same as the out-of-plane methyl groups. In **3** and **4**, the barriers to the rotation of the in-plane methyl groups are larger than the out-of-plane methyl groups by 3–4 kJ mol^{-1}, which is approximately the barrier to the rotation of the *t*-butyl group, as indicated in Table I. The difference between the barriers of the in-plane methyl group and the out-of-plane methyl groups is not as large as one might expect, considering how the strong hindrance of the H atom on the adjacent aromatic C atom might contribute to the barrier of the in-plane methyl group. To relieve this strong steric hindrance from the aromatic H atom, the rotation of the in-plane methyl group becomes coupled with the rotation of the *t*-butyl group (for which the barrier is very small in all isolated molecules of **1**–**4**). In the methyl group rotational transition state the *t*-butyl groups have rotated by 56°, 56°, 55°, and 53°, respectively, in **1**–**4** as the in-plane methyl group becomes an out-of-plane methyl group. On the other hand, rotating the *t*-butyl groups from the ground state to the transition state results in very little rotation of the in-plane methyl groups (Fig. 8 and Sec. V B 2) but rotating the in-plane methyl groups from their ground state to their transition state results in the *t*-butyl groups rotating by approximately 55°. The in-plane methyl group barriers are relieved significantly with the specific values given in Table I. These in-plane methyl group barriers are approximately the sum of the barriers of the *t*-butyl group [which, in fact must rotate over its relatively small barrier (Fig. 7)] and the out-of-plane methyl groups in **3** and **4**. The barriers for the in-plane methyl groups in **1** and **2** are even smaller than those of out-of-plane methyl groups, which is due to the greater stabilization caused by the hyperconjugation effect[13–15] in the *cis* conformation than in the *trans* conformation as discussed above.

C. Electronic structure calculations in the clusters

1. Molecular ground states in the clusters

The two-step partial structural relaxation process was applied to optimize the geometries of the clusters to obtain the ground state structures. In the optimized structure of each cluster, the orientation of the target *t*-butyl group on the home molecule agrees well with the thermal equilibrium value found in the single-crystal X-ray measurements, though other *t*-butyl groups, particularly near the edges of the clusters, assume different orientations than found in the X-ray structure. This is as expected and is not important. As discussed above in Sec. III, what is important is that the environment of the target *t*-butyl group accurately reflects the environment found in the X-ray structure.

We first deal with **1** which is unusual and, to date, unique. The asymmetric unit is half a molecule ($Z' = 1/2$), meaning that the two *t*-butyl groups are equivalent and in the *trans* conformation as opposed to the *cis* conformation as found in the isolated molecule. First, the 9 molecule cluster is built from the X-ray structure and this is shown in Fig. 2(a). Note that all molecules, in particular the orientation of all *t*-butyl groups, are identical. No calculations have been done at this point. Fig. 2(a) shows 9 identical molecules. An initial optimization of the H positions is performed and, at the scale shown in Fig. 2(a), the resulting cluster is indistinguishable from that shown. The target *t*-butyl group is indicated by the arrow in Fig. 2(a). In a first step of the calculation, when

the *intramolecular relaxation model* (where only the C and H atoms in the two *t*-butyl groups and the ring H atoms on the home molecule are allowed to structurally relax) is used with the cluster for **1**, the target *t*-butyl group already has an orientation very close to that found in the X-ray structure as presented in Sec. V A, while the other *t*-butyl group on the home molecule has rotated by 10° (from the X-ray structure). As can be seen from Fig. 2(a), the only intermolecular interactions experienced by this *t*-butyl group are from the neighboring molecules "above" and "below" it (in and out of the page in Fig. 2(a)). In the second step for **1**, the *intermolecular relaxation model is used* where the C and H atoms in all *t*-butyl groups in the cluster are allowed to relax, as well as the ring H atoms in all the molecules in the cluster. The ground state conformation of the cluster that results is shown in Fig. 2(b). Using the same convention and ordering as discussed in Sec. V A, the angles specifying the target *t*-butyl group are 96°, −23°, and −144°. These three angles all differ from the angles found in the X-ray structure by less than 1°. We conclude that the target *t*-butyl group, indicated by the arrow in Fig. 2(b), retains the orientation found in the X-ray structure. In comparing Figs. 2(a) and 2(b) it can be seen that many of the other *t*-butyl groups have reoriented. Indeed, all other *t*-butyl groups have at least part of their "surface" at the edge of the cluster. Fig. 2(c) shows a different orientation of the same structure shown in Fig. 2(b), one where it can be seen that all the slightly distorted pyrene rings are almost in the same plane. Among the 16 *t*-butyl groups on the molecules neighboring the target *t*-butyl group, one nearby *t*-butyl group is rotated by 6° (from the ground state orientation), two have rotated by 8°, and two have rotated by 13° from the X-ray (i.e., ground state) structure. The other 11 *t*-butyl groups do not show any appreciable reorientation (i.e., less than 2°). The results suggest that the clusters are large enough to account for most of the intermolecular interactions which have influence on the rotation of the target *t*-butyl group. Fig. 2(d) shows an expanded region of the central portion of Fig. 2(b) with the H atoms removed. The target molecule C atoms are indicated by beach ball atoms and the target *t*-butyl group is indicated by the "T." The distances from the quaternary C atom of the target *t*-butyl group to the quaternary C atom of several neighboring *t*-butyl groups are indicated in nm. This figure reminds us that these two-dimensional projections of the structure can be misleading. Note that there are *t*-butyl groups (one to the right of, one above [up the page], and one below [down the page] the target *t*-butyl group) that are closer to the target *t*-butyl group than the two *t*-butyl groups that appear closer in this somewhat misleading two-dimensional projection.

For **2**–**4**, we review the structures found after the *intermolecular relaxation model* is used. These are indicated in Figs. 3–5. The orientation of the target *t*-butyl groups in the clusters (indicated by arrows in Figs. 3–5) is the same as it is in the crystal as determined by the X-ray diffraction studies (Sec. V A). Other *t*-butyl groups in the clusters reorient by a few degrees by differing amounts due to the edge effect. For example, in the cluster of **2** (Fig. 3), the dihedral angle of one of the methyl groups in the target *t*-butyl group is 8°, the same as found in the single-crystal X-ray measurements, yet for some *t*-butyl groups on the edge of the clusters, the dihedral angles are 0° after the optimization, i.e., the same orientation that is found in the isolated molecule. However, the *t*-butyl groups in the optimized cluster do not necessarily adopt structures between the conformations found in the crystal and in the isolated molecule. It depends on the competition between the intramolecular and intermolecular interactions. In the case of the *t*-butyl groups on the edges of the clusters, the intermolecular interactions are absent or weak and the orientation of the *t*-butyl groups found in the isolated molecules is recovered. For those *t*-butyl groups which are neither the target *t*-butyl group nor an edge *t*-butyl group, the intermolecular interactions could be very strong and/or asymmetric. As a result, the dihedral angles of these *t*-butyl groups can assume a variety of values. In **2**, these range between 0° and 9° (with 8° being the X-ray value) and in **3** and **4**, they range between 0° and 5° (with 0° for **3** and 2° for **4** being the X-ray values). We conclude that the clusters accurately depict the environment of the target *t*-butyl groups.

2. Rotational barriers of the t-butyl groups in the clusters

We deal first with **1**. As discussed above, the orientation of each *t*-butyl group in the crystal of **1** in the ground state has one of the methyl groups oriented approximately perpendicular to the pyrene ring instead of one methyl group being coplanar with the ring as found in the isolated molecule. This is a rotation of approximately 30° from the orientation found in the isolated molecule ground state. In the transition state, one of the other methyl groups is nearly perpendicular to the ring, but on the other side of the ring. That is, if the dihedral angles for the three methyl groups in the ground state are taken to be 96°, −23°, and −144° (Sec. V C 1), then the dihedral angles in the transition state for the three methyl groups are 143°, 25°, and −95°. This is a reorientation of 47°–49° where the range reflects the additional distortion of the *t*-butyl group in the transition state. The barrier is 44.5 kJ mol^{-1} calculated using the *rigid rotation model*. When the *intramolecular relaxation model* is applied, the barrier decreases to $V_{t,\,clust}$ = 33.9 kJ mol^{-1} as reported in Tables I and III. We note that in this *intramolecular relaxation model*, the three methyl groups on the target *t*-butyl group are allowed to relax and assume their minimum energy position. The additional application of the *intermolecular relaxation model* (where all *t*-butyl groups in the cluster are allowed to relax) provides no further lowering of the barrier. The decease of the barrier is mainly caused by the reorientation of the methyl groups on the target *t*-butyl group. The methyl groups reorient by 2°, 3°, and 9° from their ground state orientations.

The rotational barriers for the target *t*-butyl group in clusters of **2**, **3**, and **4** calculated in the rigid rotation model are 29.9, 29.8, and 47.8 kJ mol^{-1}, respectively. The transition states correspond to rotations (from the ground states) of 50° in **2**, 44° in **3**, and 44° in **4** (or, rotations of 70°, 76°, and 76° in the opposite sense). Using the *intramolecular relaxation model*, followed by using the *intermolecular relaxation model*, the calculated barriers decrease to $V_{t,\,clust}$ = 15.5, 16.3, and 19.5 kJ mol^{-1} for **2**, **3** and **4**, respectively

TABLE III. NMR relaxation experimental activation energies (E) and calculated barriers (V) for *t*-butyl and constituent methyl groups in the solid state.[a]

#	Compound	E_t[b]	$V_{t,clust}$[b]	E_1[c]	$V_{1,clust}$[c]	E_2[d]	$V_{2,clust}$[e]	E_3[d]	$V_{3,clust}$[e]	NMR Refs.
1	2,7-di-*t*-butylpyrene	32(2)	33.9	13(1)	19.6	13(1)	16.6	13(1)	16.4	This work
2	1,4-di-*t*-butylbenzene	19(2)	15.5	19(2)	25.5	16(1)	18.4	16(1)	17.7	24 and 26
3	2,6-di-*t*-butylnaphthalene[f]	18(3)	16.3	18(3)	25.1	18(3)	18.4	18(3)	16.4	25
4	3-*t*-butylchrysene	24(1)	19.5	24(1)	26.0	14(1)	18.4	14(1)	17.7	23

[a]All energies are in kJ mol^{-1}.
[b]Subscript t refers to the *t*-butyl group.
[c]E_1 and $V_{1,clust}$ refer to the methyl group closest to the plane.
[d]E_2 and E_3 are always the same.
[e]$V_{2,clust}$ and $V_{3,clust}$ are ordered so $V_{2,clust} > V_{3,clust}$.
[f]Only polymorph A is considered.

(as reported in Tables I and III). In **4**, two close *t*-butyl groups on neighboring molecules reorient by 7° and 8° from their ground state orientations when the target *t*-butyl group rotates from its ground state to its transition state. In **2** and **3**, no significant reorientation of neighboring *t*-butyl groups is found to accompany the rotation of the target *t*-butyl group. Rather, the decrease in the calculated barriers when using the *partial relaxation models* (*intramolecular relaxation*, then *intermolecular relaxation*) is due to more subtle structural relaxation including the change of bond lengths and angles in the target molecule. This suggests that even though the *t*-butyl group barriers are dominated by intermolecular interactions, these same intermolecular interactions are not strong enough, or at least do not have the appropriate asymmetry, to result in coupled rotations involving *t*-butyl groups on neighboring molecules. Rather, the *t*-butyl groups adapt to the crystal packing by slightly adjusting the intramolecular structures.

3. Rotational barriers of the methyl groups in the clusters

In the isolated molecules, the methyl groups can be categorized into two "out-of-plane" methyl groups with dihedral angles of 120° and −120° (60° above and below the plane) and one "in-plane" methyl group with a dihedral angle of 0°. The two out-of-plane methyl groups are equivalent. In **2**–**4**, the orientation of the *t*-butyl groups in the clusters is similar to that found in the isolated molecules. In the cluster, the two out-of-plane methyl groups in **2**–**4** experience different intermolecular interactions because the approximate mirror plane symmetry of the isolated molecule no longer exists in the crystal. However, the transition states for all methyl groups correspond to a rotation of approximately 60° from the ground state.

In the *rigid rotation model*, the rotational barriers of the three methyl groups in **1** are 27.2, 19.5, and 19.3 kJ mol^{-1}. The methyl group 23° from its nearest plane has a higher barrier than the other two (approximately 35° and 84° from their nearest plane) because it is closer to the pyrene ring than the other two. Using the *intermolecular relaxation model* the methyl group barriers decrease to $V_{1,\,clust} = 19.6$ kJ mol^{-1}, $V_{2,\,clust} = 16.6$ kJ mol^{-1}, and $V_{3,\,clust} = 16.4$ kJ mol^{-1} as reported in Tables I and III. The number subscripts refer to the methyl groups and the barriers are ordered from largest to smallest. In the crystal of **2**, the barriers in the *rigid rotation model* are 32.6 kJ mol^{-1} for the in-plane (approximately) methyl group and 21.3 and 18.7 kJ mol^{-1} for the two out-of plane methyl groups. Using the *partial relaxation models* (*the intramolecular relaxation model* and then the *intermolecular relaxation model*) the *t*-butyl group is found to reorient by approximately 16° when the in-plane methyl group reorients from the ground state to the transition state. The barrier is $V_{1,\,clust} = 25.5$ kJ mol^{-1} for the in-plane methyl group and the barriers for the two out-of-plane methyl groups are $V_{2,\,clust} = 18.4$ kJ mol^{-1} and $V_{3,\,clust} = 17.7$ kJ mol^{-1}. These values are reported in Tables I and III.

Using the *rigid rotation model* the rotational barriers in **3** are 33.0 kJ mol^{-1} for the in-plane methyl groups and 20.8 and 19.1 kJ mol^{-1} for the out-of-plane methyl groups. These barriers for **4** are 31.6 kJ mol^{-1} for the in-plane methyl groups and 19.7 and 19.1 kJ mol^{-1} for the out-of-plane methyl groups. In the *intermolecular relaxation model*, the barriers for **3** are $V_{1,\,clust} = 25.1$ kJ mol^{-1}, $V_{2,\,clust} = 18.4$ kJ mol^{-1}, and $V_{3,\,clust} = 16.4$ kJ mol^{-1}. In the *intermolecular relaxation model*, the barriers for **4** are $V_{1,\,clust} = 26.0$ kJ mol^{-1}, $V_{2,\,clust} = 18.4$ kJ mol^{-1}, and $V_{3,\,clust} = 17.7$ kJ mol^{-1}. In **3** and **4**, there is no significant reorientation of the *t*-butyl group (<2°) when the in-plane methyl groups rotate 60° from the ground state to the transition state. The values of all the *t*-butyl group and methyl group barriers in the clusters are reported in Tables I and III. In Table I they are compared with the values in the isolated molecules and in Table III they are compared with the experimentally determined NMR activation energies presented in Sec. V D.

4. Rotation of the benzene ring in 1,4-di-t-butylbenzene (2)

In an isolated molecule of **2**, rotating the *t*-butyl group and rotating the aromatic ring are equivalent. This is no longer the case in the crystal. In all the above calculations, the aromatic C atoms were assumed to be frozen in the clusters. The assumption is probably quite good in the case of **1**, **3**, and **4** because of the large size of the aromatic rings. However, a benzene ring is much smaller and it may wobble around the thermal equilibrium position. To investigate this possibility, a 9 molecule cluster of **2** was built with a target benzene ring at the center of the cluster. The potential energy

curve for the *rigid rotation model* of the central benzene ring about the virtual C1-C4 axis (Fig. 1) was calculated at the B3LYP/6-31G(*d*) level. The thermal equilibrium orientation found in the crystal is also the ground state in this rigid potential energy surface. The transition state is the conformation with the benzene ring rotated by 90° and the barrier is very high, 373 kJ mol^{-1}. However, the potential energy surface is very flat in the vicinity of the ground state and rotating the benzene ring by 10° (8°–18°) only raises the energy by 1.6 kJ mol^{-1} and rotating it by 20° (8°–28°) only raises the energy by 14.7 kJ mol^{-1}. This suggests that the benzene ring is likely to wobble around the equilibrium orientation in the crystal. If this mode of structural relaxation were to be included in the calculation of the clusters, the computed barrier for the *t*-butyl group may decrease from the value of 15.5 kJ mol^{-1} presented in Sec. V C 2.

D. ^{1}H spin-lattice relaxation

Here, we fit the ^{1}H R versus T data presented in Fig. 6 for **1**. In addition to the four fitting parameters E_t, E_m, $\nu_{t,\infty}$, and $\nu_{m,\infty}$, we introduce the fitting parameter y in $K_i = yC_i$ for i = t, m, and tm in Eq. (3). That is, the C_i, which can be calculated, are replaced by the K_i for the fits. The model developed in Sec. IV (with explicitly calculated C values) accounts for the relaxation resulting from the modulation of the intra-*t*-butyl group ^{1}H dipolar interactions only. If the ^{1}H spins in the *t*-butyl group have dipolar interactions with other spins in the crystal *that are appreciably modulated by the rotations*, then these interactions will contribute to the observed relaxation rate. This will make $y > 1$. It is reasonable to require that all values of the C_i be increased by the same factor, so long as y is not significantly greater than unity. A fitted value of y that is significantly less than unity suggests that some aspect of the model is not correct since the interactions being accounted for are certainly present.

The fit shown in Fig. 6 (see Sec. IV) has $y = 1.00 \pm 0.03$, $E_t = 32.1^{+1.0}_{-1.9}$ kJ mol^{-1} $= 3.86^{+0.12}_{-0.23}$ kK rotor^{-1}, $E_m = 12.95^{+0.39}_{-0.78}$ kJ mol^{-1} $= 1.558^{+0.047}_{-0.094}$ kK rotor^{-1}, $\nu_{t,\infty} = (7.1^{+7.1}_{-3.6}) \times 10^{14}$ s^{-1} and $\nu_{m,\infty} = (1.09^{+1.09}_{-0.56}) \times 10^{12}$ s^{-1}. The fit cannot be significantly improved by allowing the three methyl groups to have different barriers even though this introduces many more adjustable parameters. The uncertainties in $\nu_{t,\infty}$ and $\nu_{m,\infty}$ are essentially a factor of 2. The value of $y = 1.00 \pm 0.03$ means that intra-*t*-butyl group spin-spin interactions (among the nine ^{1}H nuclei in a *t*-butyl group) dominate the spin-spin interactions. The values of E_t and $E_1 = E_2 = E_3$ are reported in Table III where they can be compared with the calculated values. A similar analysis has been performed for **2**,[24] **3**,[25] and **4**[23] and the activation energies E are reported in Table III. In **2** and **4**, $E_t = E_1$ characterize a geared motion of the *t*-butyl group and the in-plane methyl group. The other two methyl groups are characterized by another activation energy $E_2 = E_3$. Compound **3** is unusual in that all four activation energies are the same; that is, $E_t = E_1 = E_2 = E_3$.

VI. SUMMARY AND CONCLUSIONS

We have presented electronic structure calculations in four aromatic compounds with *t*-butyl groups and we have presented solid state NMR ^{1}H spin-lattice relaxation experiments in one of them. NMR relaxation experiments in the others have been reported previously. Here, we tie the results of the two techniques together to produce a model for the rotation of a *t*-butyl group and its constituent methyl groups. The compounds of interest have one or two *t*-butyl groups attached to a planar aromatic backbone. In the isolated molecules, the electronic structure calculations indicate that in the ground state the *t*-butyl groups are oriented with one methyl group in the plane of the aromatic ring with the other two methyl groups approximately 60° above and below the plane. This is probably the case for all systems similar to those studied here. In the solid state, the *t*-butyl groups in the ground state in **2**–**4** have the same orientation as they do in the isolated molecules (within a few degrees). However, in **1**, the *t*-butyl group in the solid state is oriented with one methyl group approximately 90° with respect to the aromatic plane. This is a rotation of approximately 30° from the orientation found in the isolated molecule.

The barriers for *t*-butyl group rotation in isolated molecules of **1** and **2** are ∼2 kJ mol^{-1} and those for **3** and **4** are ∼4 kJ mol^{-1}. All *t*-butyl group and methyl group barriers in the solid state are greater than 15 kJ mol^{-1} so for $100 < T < 300$ K (the temperature range of the ^{1}H spin-lattice relaxation measurements), the *t*-butyl groups can be thought of as occupying a specific ground state orientation (a potential energy minimum) and classically hopping from one potential energy minimum (absolute or local) to another. For $T < 80$ K, this model is usually inappropriate and quantum rotational tunneling should be considered. Table I summarizes the *calculated* barriers for methyl group and *t*-butyl group rotation in the four molecules investigated in this paper. The first two columns in Table I show that the barriers for the rotation of the *t*-butyl groups increase considerably in going from the isolated molecule to the crystal. This is due to the dominance of the intermolecular interactions in the solid state. We note that despite the similar molecular symmetry (and, as a consequence, the same isolated molecule *t*-butyl group barrier) in **1** and **2**, in the crystals, the *t*-butyl group barrier in **1** is twice the value that it is in **2** (and also significantly larger than the values found in **3** and **4** which are approximately the same as in **2**). This is consistent with the *t*-butyl group's unusual perpendicular geometry in **1** in which the *angular anisotropy* in the environment of the *t*-butyl groups is greater than in **2**, **3**, or **4**.

All methyl group barriers in the clusters are larger than their isolated molecule barriers (Table I) and this is generally *not* the case for systems where the methyl groups are bonded directly to the ring.[7] The calculated barriers for the out-of plane methyl groups in the crystal are 8%–27% larger than their isolated molecule values and the barriers for the in plane methyl groups in the crystal are 33%–75% larger than their isolated molecule values. Whether one considers this due to the effects of intermolecular interactions or whether one says that the intramolecular interactions have changed in

going from the isolated molecule to the solid as a consequence of the presence of intermolecular interactions is a matter of semantics since the intermolecular interactions change the geometry of the *t*-butyl group in the crystal.

The NMR spin-lattice relaxation experiments measure the magnitudes of NMR frequency Fourier components of the time-dependent magnetic fields resulting from the motion of nuclear spins (^{1}H in this case). *That's all they measure!* As ^{1}H spins move (classically) or change positions (quantum mechanically), the local magnetic fields change. In the systems of interest only *t*-butyl groups and their constituent methyl groups are moving on the appropriate NMR time scale, approximately 10^{-11}–10^{-5} s in the present case. E and ν_∞ are effective parameters in $\tau^{-1} = \nu_\infty \exp(-E/kT)$ and the model only makes sense if $E \gg kT$. This is the case for the systems in the solid state studied here. The fact that $\ln R \propto T^{-1}$ (for relaxation rate R) at both low and high temperatures means that $\tau^{-1} = \nu_\infty \exp(-E/kT)$ is valid in the sense that a more sophisticated model is not warranted. It is not surprising that the subsequent value or values of E extracted from the ^{1}H NMR spin-lattice relaxation rate data might be different than the barriers V calculated via the electronic structure calculations. Indeed, it is surprising that E and V agree so well for methyl group only rotation.[7] The simplest interpretation of the relaxation measurements for **1** is that the three methyl groups have one activation energy and the *t*-butyl group has another (higher) activation energy (Table III). The three methyl groups have the same activation energy because they are all well away from the pyrene ring. Using a more sophisticated (complicated) model would constitute an overanalysis of the data.

Table III compares the experimentally determined NMR relaxation *effective activation energies* E with the values of *barrier heights* V determined by the *ab initio* electronic structure calculations. V is uniquely defined. It is the difference between the energy of a ground state and a transition state. As discussed above, E is an average or effective energy involving the hopping or the rotation of the appropriate rotor. Both the NMR E values and the calculated V values for the three methyl groups in a *t*-butyl group are ordered $E_1 \geq E_2 \geq E_3$ and $V_1 \geq V_2 \geq V_3$ in Table III. Of the 12 methyl group barriers presented in Table III, $E < V$ in 11 cases. This is, in part, expected[11,12] since V is a barrier height whereas E is the energy difference from an effective rotational level above the minimum of the potential energy curve to an effective rotational level near or possibly slightly above the top of the barrier (the maximum of the potential energy curve). But it may also be because the calculations may be determining upper limits in some sense. In the calculations, all the ring C atoms were frozen at their X-ray values. This is fine for the rotational ground states because that is the structure that the X-ray diffraction studies provide, but perhaps some of the rotational state transition energies would be somewhat lower if the C atoms were permitted to relax. This can only be determined by extending the calculation and this will require much more computing power than is available to us at this time. For the *t*-butyl groups, $V = E$ for **1** but $E > V$ for **2**–**4**, just the opposite as is the case for the methyl groups (columns 1 and 2 in Table III). Again, the calculated V is rigorously defined. But the meaning of E for a *t*-butyl group in **2**–**4** is not clear. When a *t*-butyl group "moves" a methyl group past the ring, a classical description of the motion undoubtedly involves a subtle gearing involving both rotational and librational motions for both groups. But the solid state ^{1}H NMR spin-lattice relaxation experiments are simply not directly sensitive to fast librational motions involved with the gearing and as such the models for the motions seen by the experiments are incomplete. Indeed, for **2**–**4**, $E_t = E_1$ (the *t*-butyl group barrier equals the in-plane methyl group barrier) and this NMR activation energy should not be seen as the activation energy of the *t*-butyl group and the in-plane methyl group separately. Rather, $E_t \equiv E_1$ is a parameter that describes the coupled motion and may very well not be closely related to a barrier at all. However, for **1**, there is no methyl group in (or near) the plane and in this case, the calculated V and the observed E are the same for the *t*-butyl group.

ACKNOWLEDGMENTS

Xianlong Wang acknowledges the financial support of the National Natural Science Foundation of China (21103016) and the Research Fund for the Doctoral Program of Higher Education of China (20100185120023).

[1] R. Tilley, *Crystals and Crystal Structures* (Wiley, Chichester, UK, 2006).
[2] J. Kohanoff, *Electronic Structure Calculations for Solids and Molecules: Theory and Computational Methods* (Cambridge University Press, Cambridge, UK, 2006).
[3] R. Kimmich, *NMR Tomography, Diffusometry, Relaxometry* (Springer-Verlag, Berlin, 1997).
[4] D. P. Fahey, W. G. Dougherty, Jr., W. S. Kassel, X. Wang, and P. A. Beckmann, J. Phys. Chem. A **116**, 11946 (2012).
[5] X. Wang, L. Rotkina, H. Su, and P. A. Beckmann, ChemPhysChem **13**, 2082 (2012).
[6] P. A. Beckmann and E. Schneider, J. Chem. Phys. **136**, 054508 (2012).
[7] X. Wang, P. A. Beckmann, C. W. Mallory, A. L. Rheingold, A. G. DiPasquale, P. J. Carroll, and F. B. Mallory, J. Org. Chem. **76**, 5170 (2011).
[8] X. Wang, A. L. Rheingold, A. G. DiPasquale, F. B. Mallory, C. W. Mallory, and P. A. Beckmann, J. Chem. Phys. **128**, 124502 (2008).
[9] X. Wang, F. B. Mallory, C. W. Mallory, P. A. Beckmann, A. L. Rheingold, and M. M. Francl, J. Phys. Chem. A **110**, 3954 (2006).
[10] P. A. Beckmann, J. Rosenberg, K. Nordstrom, C. W. Mallory, and F. B. Mallory, J. Phys. Chem. A **110**, 3947 (2006) (Equation (1) should have a *d*/*dt* to the left of the left-hand side).
[11] J. Kowalewski and T. Liljefors, Chem. Phys. Lett. **64**, 170 (1979).
[12] O. Edholm and C. Blomberg, Chem. Phys. **56**, 9 (1981).
[13] V. Pophristic and L. Goodman, Nature (London) **411**, 565 (2001).
[14] I. V. Alabugin, K. M. Gilmore, and P. W. Peterson, WIREs Comput. Mol. Sci. **1**, 109 (2011).
[15] Y. Mo, WIREs Comput. Mol. Sci. **1**, 164 (2011).
[16] IUPAC, Pure Appl. Chem. **66**, 1077 (1994), see p. 1175. Also available at http://goldbook.iupac.org/V06597.html.
[17] P. A. Beckmann, C. A. Buser, C. W. Mallory, F. B. Mallory, and J. Mosher, Solid State Nucl. Mag. Reson. **12**, 251 (1998).
[18] P. A. Beckmann, K. S. Burbank, M. M. W. Lau, J. N. Ree, and T. L. Weber, Chem. Phys. **290**, 241 (2003).
[19] L. C. Popa, A. L. Rheingold, and P. A. Beckmann, Solid State Nucl. Mag. Reson. **38**, 31 (2010).
[20] P. A. Beckmann, W. G. Dougherty, Jr., and W. S. Kassel, Solid State Nucl. Mag. Reson. **36**, 86 (2009).
[21] A. L. Rheingold, A. G. DiPasquale, and P. A. Beckmann, Chem. Phys. **345**, 116 (2008).
[22] P. A. Beckmann, C. Paty, E. Allocco, M. Herd, C. Kuranz, and A. L. Rheingold, J. Chem. Phys. **120**, 5309 (2004).
[23] P. A. Beckmann, C. A. Buser, K. Gullifer, F. B. Mallory, C. W. Mallory, G. M. Rossi, and A. L. Rheingold, J. Chem. Phys. **118**, 11129 (2003).
[24] P. A. Beckmann, Phys. Rev. B **39**, 12248 (1989).

[25]P. A. Beckmann, K. S. Burbank, K. M. Clemo, E. N. Slonaker, K. Averill, C. Dybowski, J. S. Figueroa, A. Glatfelter, S. Koch, L. M. Liable-Sands, and A. L. Rheingold, J. Chem. Phys. **113**, 1958 (2000).
[26]P. A. Beckmann, F. A. Fusco, and A. E. O'Neill, J. Mag. Reson. **59**, 63 (1984).
[27]A. C. Hazell and J. G. Lomborg, Acta Cryst. B **28**, 1059 (1972).
[28]M. A. Kravers, M. Yu. Autipin, and Yu. T. Struchkov, Cryst. Struct. Commun. **9**, 955 (1980).
[29]A. L. Rheingold, J. S. Figueroa, C. Dybowski, and P. A. Beckmann, Chem. Commun. **2000**, 651 (2000).
[30]J. Klimeì and A. Michaelides, J. Chem. Phys. **137**, 120901 (2012).
[31]S. L. Price, Phys. Chem. Chem. Phys. **10**, 1996 (2008).
[32]V. L. Deringer, V. Hoepfner, and R. Dronskowski, Cryst. Growth Des. **12**, 1014 (2012).
[33]T. Steiner and W. Saenger, Acta Cryst. A **49**, 379 (1993).
[34]J. Pataki, M. Konieczny, and R. G. Harvey, J. Org. Chem. **47**, 1133 (1982).
[35]M. J. Frisch, G. W. Trucks, H. B. Schlegel *et al.*, Gaussian 09, Revision D.01, Gaussian, Inc., Wallingford, CT, 2009.
[36]D. Tzeli and A. A. Tsekouras, Chem. Phys. Lett. **496**, 42 (2010).
[37]A. Abragam, *The Principles of Nuclear Magnetism* (Oxford University Press, Oxford, 1961).
[38]P. A. Beckmann, "When is a recovery curve with noise exponential? A statistical numerical study adding random noise to exponential and stretched-exponential decay functions" (unpublished).
[39]W. I. Hembree and J. Baudry, J. Phys. Chem. B **115**, 8575 (2011).
[40]G. A. Ferguson and K. Raghavachari, J. Chem. Phys. **125**, 154708 (2006).
[41]Y. Matsumoto and K. Honma, Chem. Phys. Lett. **490**, 9 (2010).
[42]X. Wang, Ph.D. thesis, Bryn Mawr College (May, 2006).
[43]S. Tosoni, C. Tuma, J. Sauer, B. Civalleri, and P. Ugliengo, J. Chem. Phys. **127**, 154102 (2007).
[44]B. J. Lynch, Y. Zhao, and D. G. Truhlar, J. Phys. Chem. A **107**, 1384 (2003).
[45]C. Gatti, V. R. Saunders, and C. Roetti, J. Chem. Phys. **101**, 10686 (1994).
[46]M. A. Spackman and A. S. Mitchell, Phys. Chem. Chem. Phys. **3**, 1518 (2001).
[47]M. E. Foster and K. Sohlberg, Phys. Chem. Chem. Phys. **12**, 307 (2010).
[48]S. Grimme, WIREs Comput. Mol. Sci. **1**, 211 (2011).
[49]A. Otero-de-la-Roza and E. R. Johnson, J. Chem. Phys. **137**, 054103 (2012).
[50]H. Kruse and S. Grimme, J. Chem. Phys. **136**, 154101 (2012).
[51]F. Bloch, Phys. Rev. **70**, 460 (1946).
[52]N. Bloembergen, E. M. Purcell, and R. V. Pound, Phys. Rev. **73**, 679 (1948).
[53]R. K. Wangsness and F. Bloch, Phys. Rev. **89**, 728 (1953).
[54]R. Kubo and K. Tomita, J. Phys. Soc. Jpn. **9**, 888 (1954).
[55]F. Bloch, Phys. Rev. **102**, 104 (1956).
[56]F. Bloch, Phys. Rev. **105**, 1206 (1957).
[57]K. Tomita, Prog. Theor. Phys. **19**, 541 (1958).
[58] A. G. Redfield, IBM J. Res. Develop. **1**, 19 (1957); reprinted with minor revisions in A. G. Redfield, Adv. Mag. Reson. **1**, 1 (1965)
[59]I. Solomon, Phys. Rev. **99**, 559 (1955).
[60]P. S. Hubbard, Phys. Rev. **109**, 1153 (1958); **111**, 1746 (1958).
[61]D. E. Woessner, J. Chem. Phys. **36**, 1 (1962).
[62]E. O. Stejskal and H. S. Gutowsky, J. Chem. Phys. **28**, 388 (1958).
[63]R. L. Hilt and P. S. Hubbard, Phys. Rev. **134**, A392 (1964).
[64]L. K. Runnels, Phys. Rev. **134**, A28 (1964).
[65]J. D. Cutnell and W. Venable, J. Chem. Phys. **60**, 3795 (1974).
[66]A. Kumar and C. S. Johnson, Jr., J. Chem. Phys. **60**, 137 (1974).
[67]L. J. Burnett and B. H. Muller, Chem. Phys. Lett. **18**, 553 (1973).
[68]M. Mehring and H. Raber, J. Chem. Phys. **59**, 1116 (1973).
[69]M. F. Baud and P. S. Hubbard, Phys. Rev. **170**, 384 (1968).
[70]P. S. Hubbard, J. Chem. Phys. **51**, 1647 (1969).
[71]P. A. Beckmann, Mol. Phys. **41**, 1227 (1980).
[72]H. Versmold, Z. Naturforsch. A **25**, 367 (1970).
[73]W. T. Huntress, Jr., J. Chem. Phys. **48**, 3524 (1968).
[74]D. Wallach, J. Chem. Phys. **47**, 5258 (1967).
[75]S. Albert, H. S. Gutowsky, and J. A. Ripmeester, J. Chem. Phys. **56**, 3672 (1972).
[76]S. Clough and A. Heidemann, J. Phys. C: Solid State Phys. **13**, 3585 (1980).
[77]M. J. Barlow, S. Clough, A. J. Horsewill, and M. A. Mohammed, Solid State Nucl. Mag. Reson. **1**, 197 (1992).
[78]S. Clough, Physica B **136**, 145 (1986).
[79]D. Cavagnat, S. Clough, and F. O. Zelaya, J. Phys. C: Solid State Phys. **18**, 6457 (1985).
[80]S. Clough, P. J. McDonald, and F. O. Zelaya, J. Phys. C: Solid State Phys. **17**, 4413 (1984).
[81]S. Clough and P. J. McDonald, J. Phys. C: Solid State Phys. **15**, L1039 (1982).
[82]S. Clough, A. Heidemann, A. J. Horsewill, J. D. Lewis, and M. N. J. Paley, J. Phys. C: Solid State Phys. **14**, L525 (1981).
[83]C. Sun and A. J. Horsewill, Solid State Nucl. Mag. Reson. **35**, 139 (2009).
[84]A. J. Horsewill, Prog. Nucl. Mag. Reson. Spectrosc. **35**, 359 (1999).
[85]S. Clough, Solid State Nucl. Mag. Reson. **9**, 49 (1997).
[86]P. A. Beckmann, R. M. Hathorn, and F. B. Mallory, Mol. Phys. **69**, 411 (1990).